Heat stress impairs centromere structure and segregation of meiotic chromosomes in Arabidopsis

Lucie Crhak Khaitova[a], Pavlina Mikulkova[a], Jana Pecinkova[a], Manikandan Kalidass[b], Stefan Heckmann[b], Inna Lermontova[b] and Karel Riha[a,1]

[a]CEITEC Masaryk University, Brno, Czech Republic

[b]Leibniz Institute of Plant Genetics and Crop Plant Research (IPK) Gatersleben, Germany

[1]To whom correspondence should be addressed: karel.riha@ceitec.muni.cz

Abstract

Heat stress is a major threat to global crop production, and understanding its impact on plant fertility is crucial for developing climate-resilient crops. Despite the known negative effects of heat stress on plant reproduction, the underlying molecular mechanisms remain poorly understood. Here, we investigated the impact of elevated temperature on centromere structure and chromosome segregation during meiosis in *Arabidopsis thaliana*. Our findings reveal that heat stress causes a significant decline in fertility and leads to the formation of micronuclei in pollen mother cells, along with an extended duration of meiotic division. We also demonstrate a reduction in the amounts of centromeric histone and the kinetochore protein BMF1 at meiotic centromeres with increasing temperature. Furthermore, we show that heat stress prolongs the activity of the spindle assembly checkpoint during meiosis I, indicating impaired efficiency of the kinetochore attachments to spindle microtubules. Our analysis of mutants with reduced amounts of centromeric histone suggests that weakened centromeres sensitize plants to elevated temperature, resulting in meiotic defects and reduced fertility even at moderate temperatures. These results indicate that the structure and functionality of meiotic centromeres in *Arabidopsis* are highly sensitive to heat stress, and suggest that centromeres and kinetochores may represent a crucial bottleneck in plant adaptation to increasing temperatures.

Introduction

Global warming impacts crop productivity with more frequent and extreme heatwaves being particularly damaging (1). The lower yields associated with heatwaves are mainly attributed to the impairment of the plant reproductive system (2). Thus, a fundamental understanding of how heat stress affects plant reproduction can guide breeding strategies towards generating climate change resilient crops. Heat stress impairs both male and female reproductive structures, but male gametogenesis is particularly sensitive to higher temperatures (3). Studies in crop and non-crop species have shown that heat stress affects pollen count, morphology, viability, dehiscence, germination and pollen tube growth (4, 5).

Acute heat stress applied at different stages of flower development has been found to have the most detrimental effect during microsporogenesis (6, 7). Meiosis, a reductive cell division that halves number of chromosomes in two consecutive rounds of chromosome segregation, is a crucial step of microsporogenesis. It is a relatively slow process, lasting approximately 1.5 to 2 days in Arabidopsis and barley (8-11). Prophase I, the longest phase of meiosis, is characterized by pairing and recombination of homologous chromosomes to form stable bivalents. It is followed by two chromosome segregation cycles that first divide homologous chromosomes and then the sister chromatids. Heat stress affects various aspects of plant meiosis. In prophase I, elevated temperature alters the rate and distribution of meiotic recombination (10, 12, 13) and a recent study in Arabidopsis has shown that heat shock response pathway directly regulates the recombination machinery (14). More severe heat stress can impair synapsis and pairing of homologous chromosomes (15-17). This is likely due to inefficient completion of homologous recombination, which is monitored by specialized pachytene checkpoint (18).

Heat stress affects the later stages of meiosis as well. Elevated temperatures disturb spindle orientation during meiotic divisions and the formation of radial microtubule arrays, resulting in aberrant cytokinesis and diploid microspores (7, 16). Furthermore, acute heat stress leads to chromosome mis-segregation and the formation of micronuclei (16, 18, 19). The meiotic micronuclei and chromosomal aberrations may arise as a consequence of abnormal repair of meiotic DNA breaks or homologous recombination intermediates in prophase I. However, they can also be caused by defects in chromosome segregation during meiotic divisions (20). Proper attachment of kinetochores to the spindle microtubules before anaphase is crucial

for faithful chromosome partitioning to daughter cells, and this process is controlled by spindle assembly checkpoint. Therefore, micronuclei typically occur in mutants with impaired centromere/kinetochore structure or spindle assembly checkpoint (SAC) when treated with spindle inhibitors (21, 22).

In most eukaryotes centromeres are confined to a restricted region on each chromosome that serves as a platform for assembly of the kinetochore, a multiprotein structure that connects chromosome with the spindle. Centromeres are defined epigenetically by a specialized centromeric histone H3 variant (CENH3), which forms the foundation for the recruitment of kinetochore proteins (23). In contrast to canonical histones, replicative dilution of CENH3 is not replenished immediately in S-phase, but in subsequent stages of the cell cycle (24). In plants, CENH3 is loaded on centromeres in G2 and persists there throughout the cell cycle (25, 26). CENH3 is a very stable component of centromeric chromatin, although its amount at centromeres gradually declines in terminally differentiated cells in plants and animals (27, 28).

In this study, we have discovered that heat stress significantly reduces the amount of CENH3 on meiotic chromosomes in *Arabidopsis thaliana*. This loss of CENH3 leads to the formation of micronuclei, which in turn contributes to the decrease in pollen formation and fertility in plants exposed to heat stress. Additionally, we have found that plants with a genetic mutation that reduces the amount of centromeric histone are more sensitive to moderately elevated temperature. These results suggest that meiotic centromeres may represent a crucial point of vulnerability for plants in adaptation to raising temperatures.

Results

Pollen production and fertility decline with increasing temperature

In our previous work, we identified the *cenh3-4* allele of Arabidopsis centromeric histone *CENH3* that carries a mutation in the splicing donor site of the 3rd exon (29). This leads to a 10-fold reduction in fully spliced *CENH3* mRNA and a decreased amount of centromeric histone. Consequently, *cenh3-4* plants have smaller centromeres and are sensitive to oryzalin (29). Under standard conditions, *cenh3-4* mutants are barely distinguishable from wild type, but we noticed their reduced fertility when grown at an elevated temperature. To systematically assess this phenotype, we grew plants under standard conditions (21°C) until

they formed four true leaves, and then continued their cultivation in growth chambers tempered to 16, 21, 26 and 30°C (Figure S1). At 16°C, plants exhibited the slowest growth, but also the highest fertility, as assessed by pollen count and silique length, which is indicative of seed yield (Figure 1). Fertility slightly decreased at 21°C and further declined at 26°C. In *cenh3-4* mutants, we noticed a sharp decline in pollen production and fertility at 26°C (86±48 pollen per anther), whereas the fertility of the wild type was still relatively high (213±58 pollen per anther) (Figure 1B,C). Both *cenh3-4* and wild type plants became infertile at 30°C. The heat-induced sterility was reversible and *cenh3-4* as well as wild type plants transferred from 30 to 21°C regained fertile flowers (Figure S1C). These data indicate that pollen production and fertility gradually decline with increasing temperature and this trend is particularly pronounced in *cenh3-4* mutants that have become almost sterile already at 26°C.

It has been reported that extreme heat stress alters chromosome segregation fidelity and the duration of Arabidopsis meiosis (18). Temperatures of 34°C and above abolished chromosome pairing and synapsis and led to the formation of univalents. However, meiotic chromosomes are fully paired at 30°C (17, 18, 30) indicating that the recombination defects are not primarily responsible for abortive pollen development at this temperature.

Heat stress delays meiotic progression and induces micronuclei

To assess the effect of temperature on meiotic progression and chromosome segregation at temperatures up to 30°C, we performed live imaging of meiotic divisions in the HTA10:RFP reporter line, which marks chromatin (11). We measured the duration of meiotic divisions from the end of diakinesis until the formation of haploid nuclei in telophase II (Figure S2). Meiotic divisions were slowest at 16°C and lasted, on average, 441 and 459 min in wild type and *cenh3-4*, respectively (Movies 1 and 2, Figure 2A). Meiosis progressed significantly faster with increasing temperature. Wild type meiotic divisions took 169 min at 21°C and 142 min at 26°C (Movies 3 and 4). Meiotic divisions were also rapid in *cenh3-4* at 21°C, lasting on average 156 min, but slowed down to 238 min at 26°C (Movies 5 and 6). This contrasts with the situation in wild type, where divisions occur at the fastest rate at 26°C. Interestingly, meiotic divisions were prolonged at 30°C in both wild type and *cenh3-4* mutants to 286 and 264 min, respectively (Movies 7 and 8). The slowdown of meiosis at 26°C and 30°C in *cenh3-*

4, and at 30°C in wild type coincides with the steep decline of pollen production (Figure 1B,C) and indicates problems with meiotic progression.

Live imaging in *cenh3-4* plants and, at 30°C, also in wild type showed formation of micronuclei that began to form during meiosis I and persisted till telophase II (Movies 7 and 8). We quantified the micronuclei in fixed anthers at the tetrad stage using confocal microscopy (Figure 2B,C). The micronuclei were apparent in *cenh3-4* mutants at all temperatures, which is consistent with partially impaired centromere function in these plants (29). Nevertheless, their occurrence substantially increased at 26°C and severe defects in chromosome segregation were observed at 30°C (Figure 2B,C; Movies 6 and 8) resulting in very few regular tetrads. Whereas we occasionally detected micronuclei at lower temperatures also in wild type, albeit at a much lower level than in *cenh3-4*, their incidence increased 15-fold between 26°C and 30°C (Figure 2B,C, Movies 4 and 7). In addition, we observed dyads and polyads, which is consistent with the previous study performed at a similar temperature (16). These data show that temperature-induced fertility reduction coincides with increased occurrence of micronuclei.

Micronuclei may arise from acentric fragments and dicentric chromosomes derived from defective repair of meiotic breaks. Indeed, temperatures above 30°C were reported to cause aberrant recombination intermediates and induce pachytene checkpoint (16, 18). In this scenario, the absence of meiotic breaks in SPO11-deficient plants should prevent the formation of temperature-induced micronuclei. Arabidopsis *spo11-2* mutants do not form bivalents, and homologous chromosomes segregate randomly in anaphase I (31, 32). Cytogenetic analysis in *spo11-2* plants revealed a relatively high level of micronuclei in tetrads at 21°C (Figure 2B,C). Because unpaired univalents cannot properly bi-orient at metaphase I spindle, these micronuclei are likely generated by chromosome mis-segregation. Importantly, number of the micronuclei almost doubled in *spo11-2* plants grown at 30°C (Figure 2B,C) arguing that temperature has a direct effect on chromosome segregation.

In its natural habitats, *A. thaliana* usually flowers from March to early summer under average daily temperatures lower than the ones used for cultivation in laboratories (33, 34). Due to the day-night cycle, they never experience sustained temperatures over 30°C. Therefore, we tested whether meiotic defects observed after continuous cultivation at 30°C

could also be induced under more physiological conditions that mimic a hot day. To this end, we cultivated plants in chambers tempered to 18°C overnight and increased temperature to 34°C for 6 hrs during the day (Figure S3A). We observed a drastic reduction in fertility and pollen count, as well as an increased frequency of micronuclei compared to control plants grown under the 18°C/21°C night/day regime (Figure S3B-D). These data suggest that heatwaves occurring during flowering can have a detrimental effect on Arabidopsis meiosis.

Heat stress reduces the amounts of centromeric histone on meiotic centromeres

Our phenotypic analysis indicates that *cenh3-4* mutants grown at 26°C exhibit the same behavior as wild type plants grown at 30°C. Therefore, we investigated whether increasing temperature weakens the centromere structure, which could explain the temperature sensitivity of *cenh3-4* plants with less centromeric histone. CENH3 is present on meiotic chromosomes from early prophase I (25, 26) and its signal is most visible in pachytene when homologous chromosomes are fully synapsed. To evaluate the effect of temperature on centromeres, we analyzed the CENH3 signal on pachytene chromosomes in anthers of the Arabidopsis *eYFP:CENH3* reporter line (35, 36) grown at 21, 26 and 30°C. While eYFP:CENH3 was easily detectable on pachytene chromosomes at 21°C, the signal decreased significantly at 26°C and declined further at 30°C (Figure 3A,B). We observed this trend in three independent experiments (Figure 3B). In contrast, the eYFP:CENH3 signal in tapetum nuclei neighboring the pollen mother cells exhibited the opposite trend and increased with elevated temperature (Figure 3A,C). This resulted in a striking difference in signal intensity at 30°C, where the tapetum exhibited a strong eYFP:CENH3 signal, whereas the signal on pachytene chromosomes in the same field of view was barely detectable (Figure 3A).

CENH3 acts as a platform for binding additional kinetochore and spindle assembly checkpoint proteins. BMF1 is an Arabidopsis BUB1-related protein that associates with centromeres throughout the cell cycle (37). We generated Arabidopsis marker lines expressing *BMF1::BMF1:eYFP* and *BMF1::BMF1:TagRFP* constructs, and validated BMF1 co-localization with CENH3 from early prophase I until telophase II (Figure S4, Movie 9). Quantification of the BMF1:eYFP signal on pachytene chromosomes showed a decline at 26°C, and BMF1 was undetectable at 30°C (Figure 3D,E). These data suggest that elevated temperature reduces the amount of CENH3 and the kinetochore protein BMF1 on meiotic centromeres, potentially affecting their functionality.

Heat stress prolongs spindle assembly checkpoint in metaphase I

In our previous report, we showed that reduced amount of CENH3 and smaller centromeres prolonged the biorientation of mitotic chromosomes in *cenh3-4* plants (29). Biorientation is monitored by the spindle assembly checkpoint (SAC), and its satisfaction triggers anaphase. We hypothesized that meiotic chromosomes with heat-induced reductions in CENH3 might take longer to properly attach to the spindle and satisfy the SAC. The core SAC proteins temporarily associate with the kinetochore during spindle formation and disappear shortly before the onset of anaphase. BMF3 is one of the core components of the Arabidopsis SAC that associates with the kinetochore during prometaphase and extends this association in the presence of a spindle inhibitor (37). To monitor SAC on meiotic chromosomes, we generated an Arabidopsis line expressing *BMF3::BMF3:GFP* together with the tubulin marker TagRFP:TUB4. Initially, we validated the localization of BMF3 on meiotic chromosomes by live cell imaging since BMF3 was previously only analyzed in the context of mitosis (37). We observed the BMF3:GFP signal during prometaphase/metaphase I, it disappeared at the onset of anaphase I and reappeared again during metaphase II indicating that BMF3 is a component of the meiotic SAC (Figure 4A, Movie 10). We then analyzed the effect of temperature on SAC duration. Since the signal was more prominent in metaphase I, we measured the duration of the active SAC during meiosis I. We observed that while the BMF3:GFP signal persisted, on average, for about 22.7 min at 21 and 26°C, its appearance was prolonged to 40.5 min at 30°C (Figure 4B, Movies 11 and 12). This observation supports our finding that centromere structure is compromised at elevated temperatures, which may extend the time necessary for chromosome biorientation.

Discussion

In this study we investigated the impact of increased temperature on fertility and meiotic progression in Arabidopsis. We observed that *A. thaliana* (ecotype Col-0) exhibited the highest fertility when grown at 16°C, which closely resembles the average temperature during flowering in its natural habitats (34). At this temperature, meiotic divisions took more than twice as long as at 21°C. Arabidopsis grown at 17°C was reported to exhibit slower microsporogenesis, with the entire meiosis process lasting 48 hours as opposed to 32 hours at 24°C (38). Interestingly, the slower progression was found to be less detrimental for several mutations that affect microsporogenesis, indicating that a slower pace provides

greater robustness. Overall, these observations suggest that the pace of meiosis in Arabidopsis is well optimized for its natural growth conditions, enabling the plants to achieve maximum fitness.

The process of meiosis is progressively accelerated with increasing temperature (18) (Figure 2). However, the speed of meiotic divisions reaches its maximum at 26°C and slows down at 30°C under the conditions used in this study. At 30°C, fertility is lost and high incidence of micronuclei is observed, implying that the temperature around 30°C impairs some molecular processes involved in chromosome segregation and genome integrity. The micronuclei can represent acentric fragments derived from aberrant processing of recombination intermediates. Indeed, the impact of temperature on recombination machinery is well documented. A moderate increase in temperature leads to shift in chiasma distribution and cross-over frequency (10, 12, 13). Heat stress above 30°C severely impairs recombination and synapsis, leading to univalents and chromosome segregation defects (16-18, 30). Nevertheless, we observed an increased incidence of micronuclei also in SPO11-deficient plants that do not form meiotic DNA double-strand breaks indicating that only a portion of micronuclei is derived from aberrant recombination.

Micronuclei can also be formed by aberrant chromosome segregation during anaphase (20). The accurate partitioning of chromosomes depends on the correct attachment of centromeres to the spindle microtubules. Recent reports have indicated that the stability of microtubules in plant meiocytes is compromised by heat stress (18, 19). In this study, we have demonstrated that high temperature also affects the structure and function of meiotic centromeres. Our findings suggest that elevated temperature reduces the amount of CENH3 and BMF1 on meiotic centromeres (Figure 3). These weakened centromeres may be less effective in establishing productive interactions with spindle microtubules. This is consistent with the prolonged spindle assembly checkpoint we observed through the longer residency of BMF3 on prometaphase I centromeres at 30°C (Figure 4). Taken together, our data indicate that heat stress impairs centromere function, which in turn decreases the efficiency of proper attachment of chromosomes to the meiotic spindle. As a result, these chromosomes may not be transported to their intended destination in a timely manner and, therefore, not incorporated into the newly formed nuclei. This scenario also explains the

increased temperature-sensitivity of *cenh3-4* plants, which already have smaller centromeres (29); even moderately elevated temperature may further enhance this defect.

How elevated temperature affects the amount of CENH3 on centromeres? Studies in human cells have revealed that CENH3 nucleosomes are less stable than previously thought. The amount of CENH3 at centromeres declines over time and must be actively replenished to preserve centromere identity and proliferative potential (28). Transcription has been shown to cause the eviction of pre-existing CENH3 from the centromeres (28). In Arabidopsis, depletion of CENH3 from centromeres has been observed in leaf cells with increasing age, indicating that this phenomenon also occurs in plants (27). The Arabidopsis centromeric satellite repeat CEN180 undergoes pervasive transcription, which is largely repressed by epigenetic silencing mechanisms (39). However, heat stress can alleviate the repression and induce transcription of CEN180 from silent loci (40). This temperature-induced transcription can increase the eviction of CENH3 nucleosomes, potentially compromising centromere structure if not replenished. Interestingly, in contrast to pollen mother cells, tapetum cells do not exhibit CENH3 loss at elevated temperatures (Figure 3C). This may be due to the different efficiency of CENH3 deposition to replenish the heat-induced loss of CENH3 in these cell types. Accordingly, Arabidopsis meiotic cells possess a specialized CENH3 loading mechanism that seems more stringent than the loading mechanism operating in mitotic cells (21, 41, 42).

Crosses between wild type and plants with altered CENH3 can result in postzygotic loss of one set of parental chromosomes (43). This is attributed to inefficient re-loading of CENH3 on the set of parental chromosomes with the altered centromeres in hybrid embryos (44). Recent studies showed that heat stress applied during early embryogenesis could enhance the centromere-mediated genome elimination in Arabidopsis (45, 46). This indicates that similarly to meiocytes, elevated temperature can also destabilize centromeres in embryonic cells.

In conclusion, our study highlights the significant impact of temperature on the centromere structure and reproduction in Arabidopsis. We found that already moderate increase in temperature has a discernable effect on pollen production and silique length, and exposure to 30°C impairs the structure of centromeres and leads to plant sterility. These findings are particularly relevant in the context of climate change, where rising temperatures and more

frequent weather extreme periods pose a threat to global food security by disrupting plant reproductive processes. As such, our study provides important insights into the mechanisms that contribute to the reduction of plant fertility in response to elevated temperature. Further research on molecular aspects underlying these effects may help to develop strategies to generate plants more resilient to extreme weather during their reproductive phase.

Material and Methods

Plant material and growth conditions

Arabidopsis thaliana ecotype Columbia (Col-0), *cenh3-4* (29) and *spo11-2-3* (32) seeds were grown on soil in growth chambers at 21°C, 16 h/8 h light/dark cycles and 50% of humidity until the 1.04 growth stage. Plants were then transferred to different chambers with continuous 16, 21, 26, 30°C or 34°C/18°C and 21°C/18°C at 16 h/8 h light/dark cycles and 50% of humidity. Plants used for live cell imaging were generated by crossing *HTA10:RFP* (11) and *pRPS5A::TagRFP:TUB4* (9) reporter lines with *cenh3-4* mutant and *BMF3::BMF3:GFP* reporter line, respectively. *eYFP:CENH3* reporter line was described and characterized in previous studies (35, 36).

Generating reporter lines

To generate the BMF1 and BMF3 reporter lines, we amplified the promoter and genomic regions of BMF1 using the primers CACCTGAGTCTCCAACGTTA and CGAAGAGCATAACGAGATGCG. The PCR products were then cloned into the destination vectors pGWB659 and pGWB640, respectively, to create marker lines tagged with TagRFP and eYFP at the C-terminus. Similarly, we amplified the BMF3 promoter and genomic regions using the primers CACCATGCAGATGGTCCTCC and GAAGTCCATTGGCATTGCAAA, and subcloned them into the pGWB650 destination vector using gateway cloning to generate the *BMF3::BMF3:GFP* line. We then introduced these constructs into wild-type plants using Agrobacterium-mediated floral dip transformation. We used non-segregating homozygous transgenic lines for microscopic analyses.

Assessment of plant fertility

Pollen viability was determined by Alexander staining (47). Anthers were imaged using Zeiss Axioscope A1 equipped with 20x/0.5 objective (Zeiss) and processed in Zeiss ZEN software. Silique length was assessed from images of main stems scanned by an Epson scanner and the siliques were measured using the Fiji Analyze/Measure function (48).

Cytology

To examine micronuclei, DAPI staining of PMCs was used in whole anther as described (29). Anthers were imaged using Zeiss LSM780 confocal microscope (63X/1.4 oil objective) and image processing was done using Zeiss ZEN software (Zeiss). To quantify the fluorescence signal intensity of eYFP:CENH3 and BMF1:eYFP, anthers were DAPI stained as described above, and Z-stacks were acquired using Zeiss LSM880 confocal microscope equipped with the Fast module 32-channels Airyscan detector (63x/1.4 oil objective). The fluorescence intensity was quantified using Fiji (48) according to the procedure described by Shihan et al. (49). This involved generating a SUM of signal in z-stacks covering one nucleus, background subtraction, and measuring Raw Integral Density per one signal. This process was repeated individually in each nucleus.

Live cell imaging

Live cell imaging of meiosis was performed by light-sheet fluorescent microscopy using Light-sheet Z.1 microscope (Zeiss) as previously described (11, 29). Imaging of male meiosis was conducted using 10x or 20x objectives (Detection optics 10x/0.5 or 20x/1.0), single illumination (Illumination Optics 10x/0.2) and two track imaging with 488 nm laser for GFP and eYFP, and 561 nm laser for RFP, in 5 min time increments. Imaging of BMF3:GFP and TagRFP:TUB4 markers for SAC analysis was performed using fast scanning in 1 min time increments. Images were deconvolved with a Regularized Inverse Filter and further processed in Zeiss ZEN software for Light-sheet (Zeiss). To correct occasional sample drift, the Correct 3D drift plugin in Fiji (50) was used.

Acknowledgements

We acknowledge the support from CEITEC MU Core facilities Plant Sciences and CELLIM, supported by the Czech-Bioimaging (No. LM2018129) infrastructure project funded by MEYS CZ. This work was

funded by the Czech Science Foundation (grant 21-25163J to K.R.). MK is supported by Deutsche Forschungsgemeinschaft (LE2299/5–1).

Literature

1. T. A. Bras, J. Seixas, N. Carvalhais, J. Jagermeyr, Severity of drought and heatwave crop losses tripled over the last five decades in Europe. *Environ Res Lett* **16** (2021).
2. R. Lippmann, S. Babben, A. Menger, C. Delker, M. Quint, Development of Wild and Cultivated Plants under Global Warming Conditions. *Curr Biol* **29**, R1326-R1338 (2019).
3. K. E. Zinn, M. Tunc-Ozdemir, J. F. Harper, Temperature stress and plant sexual reproduction: uncovering the weakest links. *J Exp Bot* **61**, 1959-1968 (2010).
4. P. Chaturvedi *et al.*, Heat stress response mechanisms in pollen development. *New Phytol* **231**, 571-585 (2021).
5. N. De Storme, D. Geelen, The impact of environmental stress on male reproductive development in plants: biological processes and molecular mechanisms. *Plant Cell Environ* **37**, 1-18 (2014).
6. A. Hedhly, A. Nestorova, A. Herrmann, U. Grossniklaus, Acute heat stress during stamen development affects both the germline and sporophytic lineages in Arabidopsis thaliana (L.) Heynh. *Environ Exp Bot* **173** (2020).
7. Y. Pecrix *et al.*, Polyploidization mechanisms: temperature environment can induce diploid gamete formation in Rosa sp. *Journal of Experimental Botany* **62**, 3587-3597 (2011).
8. S. J. Armstrong, F. C. H. Franklin, G. H. Jones, A meiotic time-course for Arabidopsis thaliana. *Sex Plant Reprod* **16**, 141-149 (2003).
9. M. A. Prusicki *et al.*, Live cell imaging of meiosis in Arabidopsis thaliana. *Elife* **8** (2019).
10. J. D. Higgins *et al.*, Spatiotemporal asymmetry of the meiotic program underlies the predominantly distal distribution of meiotic crossovers in barley. *Plant Cell* **24**, 4096-4109 (2012).
11. S. Valuchova *et al.*, Imaging plant germline differentiation within Arabidopsis flowers by light sheet microscopy. *Elife* **9** (2020).
12. A. Lloyd, C. Morgan, H. F. FC, K. Bomblies, Plasticity of Meiotic Recombination Rates in Response to Temperature in Arabidopsis. *Genetics* **208**, 1409-1420 (2018).
13. J. L. Modliszewski *et al.*, Elevated temperature increases meiotic crossover frequency via the interfering (Type I) pathway in Arabidopsis thaliana. *PLoS Genet* **14**, e1007384 (2018).
14. J. Kim *et al.*, Arabidopsis HEAT SHOCK FACTOR BINDING PROTEIN is required to limit meiotic crossovers and HEI10 transcription. *EMBO J* **41**, e109958 (2022).

15. J. Loidl, Effects of elevated temperature on meiotic chromosome synapsis in Allium ursinum. *Chromosoma* **97**, 449-458 (1989).

16. N. De Storme, D. Geelen, High temperatures alter cross-over distribution and induce male meiotic restitution in Arabidopsis thaliana. *Commun Biol* **3**, 187 (2020).

17. Y. Ning *et al.*, Heat stress interferes with formation of double-strand breaks and homolog synapsis. *Plant Physiol* **185**, 1783-1797 (2021).

18. J. De Jaeger-Braet, L. Krause, A. Buchholz, A. Schnittger, Heat stress reveals a specialized variant of the pachytene checkpoint in meiosis of Arabidopsis thaliana. *Plant Cell* **34**, 433-454 (2022).

19. J. Wang, D. Li, F. Shang, X. Kang, High temperature-induced production of unreduced pollen and its cytological effects in Populus. *Sci Rep* **7**, 5281 (2017).

20. M. Fenech *et al.*, Molecular mechanisms of micronucleus, nucleoplasmic bridge and nuclear bud formation in mammalian and human cells. *Mutagenesis* **26**, 125-132 (2011).

21. I. Lermontova *et al.*, Knockdown of CENH3 in Arabidopsis reduces mitotic divisions and causes sterility by disturbed meiotic chromosome segregation. *Plant J* **68**, 40-50 (2011).

22. P. Kalitsis, E. Earle, K. J. Fowler, K. H. Choo, Bub3 gene disruption in mice reveals essential mitotic spindle checkpoint function during early embryogenesis. *Genes Dev* **14**, 2277-2282 (2000).

23. A. D. McAinsh, A. L. Marston, The Four Causes: The Functional Architecture of Centromeres and Kinetochores. *Annu Rev Genet* **56**, 279-314 (2022).

24. A. Stirpe, P. Heun, The ins and outs of CENP-A: Chromatin dynamics of the centromere-specific histone. *Semin Cell Dev Biol* **135**, 24-34 (2023).

25. P. B. Talbert, R. Masuelli, A. P. Tyagi, L. Comai, S. Henikoff, Centromeric localization and adaptive evolution of an Arabidopsis histone H3 variant. *Plant Cell* **14**, 1053-1066 (2002).

26. I. Lermontova *et al.*, Loading of Arabidopsis centromeric histone CENH3 occurs mainly during G2 and requires the presence of the histone fold domain. *Plant Cell* **18**, 2443-2451 (2006).

27. I. Lermontova, T. Rutten, I. Schubert, Deposition, turnover, and release of CENH3 at Arabidopsis centromeres. *Chromosoma* **120**, 633-640 (2011).

28. S. Z. Swartz *et al.*, Quiescent Cells Actively Replenish CENP-A Nucleosomes to Maintain Centromere Identity and Proliferative Potential. *Dev Cell* **51**, 35-48 e37 (2019).

29. C. Capitao *et al.*, A CENH3 mutation promotes meiotic exit and restores fertility in SMG7-deficient Arabidopsis. *PLoS Genet* **17**, e1009779 (2021).

30. H. Fu *et al.*, Interfered chromosome pairing at high temperature promotes meiotic instability in autotetraploid Arabidopsis. *Plant Physiol* **188**, 1210-1228 (2022).

31. N. J. Stacey *et al.*, Arabidopsis SPO11-2 functions with SPO11-1 in meiotic recombination. *Plant J* **48**, 206-216 (2006).

32. F. Hartung *et al.*, The catalytically active tyrosine residues of both SPO11-1 and SPO11-2 are required for meiotic double-strand break induction in Arabidopsis. *Plant Cell* **19**, 3090-3099 (2007).

33. C. Shindo, G. Bernasconi, C. S. Hardtke, Natural genetic variation in Arabidopsis: tools, traits and prospects for evolutionary ecology. *Ann Bot* **99**, 1043-1054 (2007).

34. B. Brachi *et al.*, Linkage and association mapping of Arabidopsis thaliana flowering time in nature. *PLoS Genet* **6**, e1000940 (2010).

35. S. Le Goff *et al.*, The H3 histone chaperone NASP(SIM3) escorts CenH3 in Arabidopsis. *Plant J* **101**, 71-86 (2020).

36. D. Demidov *et al.*, Haploid induction by nanobody-targeted ubiquitin-proteasome-based degradation of EYFP-tagged CENH3 in Arabidopsis thaliana. *J Exp Bot* **73**, 7243-7254 (2022).

37. S. Komaki, A. Schnittger, The Spindle Assembly Checkpoint in Arabidopsis Is Rapidly Shut Off during Severe Stress. *Dev Cell* **43**, 172-185 e175 (2017).

38. J. Zhu *et al.*, Slowing development restores the fertility of thermo-sensitive male-sterile plant lines. *Nat Plants* **6**, 360-367 (2020).

39. B. P. May, Z. B. Lippman, Y. Fang, D. L. Spector, R. A. Martienssen, Differential regulation of strand-specific transcripts from Arabidopsis centromeric satellite repeats. *PLoS Genet* **1**, e79 (2005).

40. M. Tittel-Elmer *et al.*, Stress-induced activation of heterochromatic transcription. *PLoS Genet* **6**, e1001175 (2010).

41. M. Ravi *et al.*, Meiosis-specific loading of the centromere-specific histone CENH3 in Arabidopsis thaliana. *PLoS Genet* **7**, e1002121 (2011).

42. V. Schubert, I. Lermontova, I. Schubert, Loading of the centromeric histone H3 variant during meiosis-how does it differ from mitosis? *Chromosoma* **123**, 491-497 (2014).

43. M. Ravi, S. W. Chan, Haploid plants produced by centromere-mediated genome elimination. *Nature* **464**, 615-618 (2010).

44. M. P. A. Marimuthu *et al.*, Epigenetically mismatched parental centromeres trigger genome elimination in hybrids. *Sci Adv* **7**, eabk1151 (2021).

45. U. Ahmadli *et al.*, High temperature increases centromere-mediated genome elimination frequency and enhances haploid induction in Arabidopsis. *Plant Commun* 10.1016/j.xplc.2022.100507, 100507 (2022).

46. C. Jin, L. Sun, H. K. Trinh, G. Danny, Heat stress promotes haploid formation during CENH3-mediated genome elimination in Arabidopsis. *Plant Reproduction* 10.1007/s00497-023-00457-8 (2023).

47. M. P. Alexander, Differential Staining of Aborted and Nonaborted Pollen. *Stain Technol* **44**, 117-+ (1969).

48. J. Schindelin *et al.*, Fiji: an open-source platform for biological-image analysis. *Nat Methods* **9**, 676-682 (2012).

49. M. H. Shihan, S. G. Novo, S. J. Le Marchand, Y. Wang, M. K. Duncan, A simple method for quantitating confocal fluorescent images. *Biochem Biophys Rep* **25**, 100916 (2021).

50. A. Parslow, A. Cardona, R. J. Bryson-Richardson, Sample drift correction following 4D confocal time-lapse imaging. *J Vis Exp* 10.3791/51086 (2014).

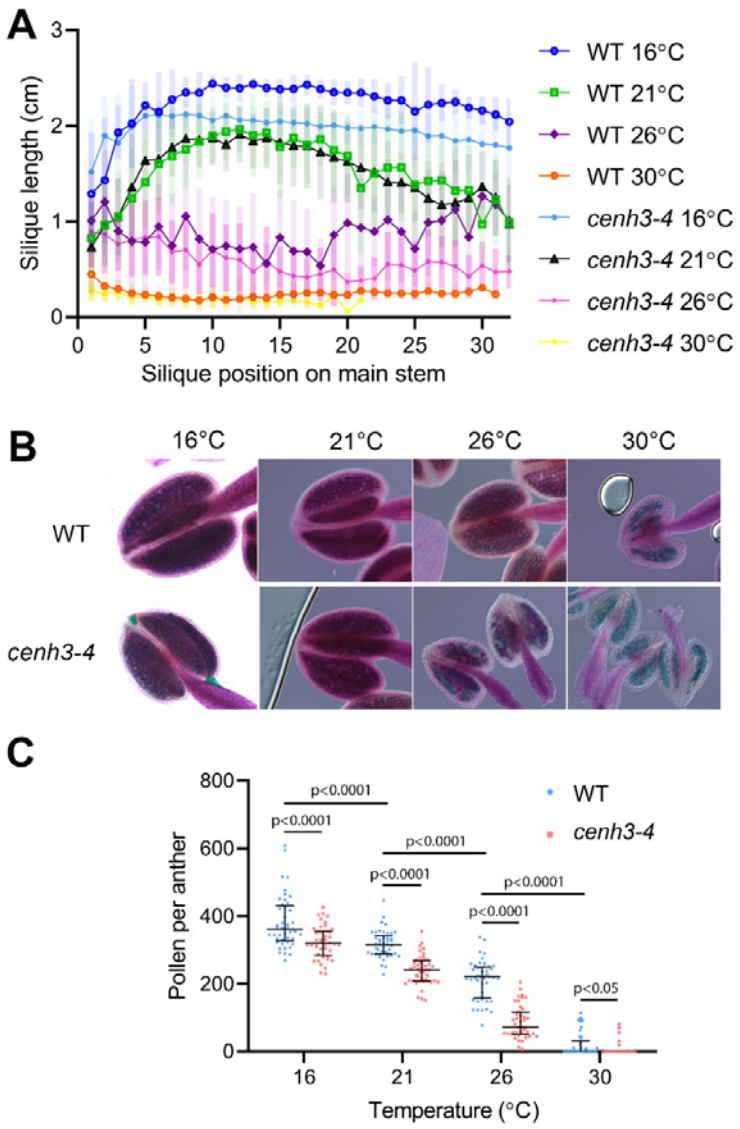

Figure 1. Effect of temperature on fertility in wild type and *cenh3-4* plants.

(A) Analysis of silique length through the main stem of wild type (WT) grown at 16°C (n=18), 21°C (n=25), 26°C (n=13), 30°C (n=20) and *cenh3-4* mutant at 16°C (n=22), 21°C (n=20), 26°C (n=22) and 30°C (n=11). The silique position is numbered from the oldest to the youngest silique on the main stem. Error bars depict standard deviation. (B) Anthers of the abovementioned plants after Alexander staining. (C) Quantification of viable pollen per anther (n=45). Significance of the difference is counted using Two-tailed t-test.

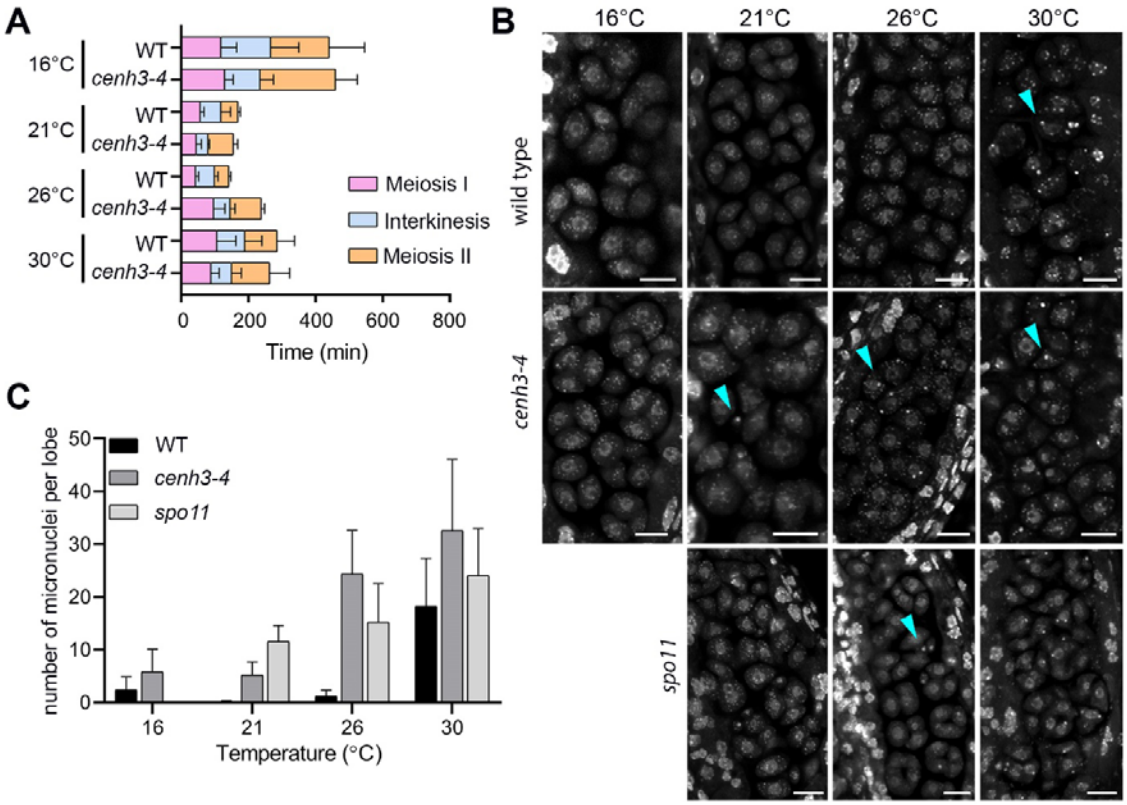

Figure 2. Effect of temperature on meiosis duration and micronuclei formation.

(A) Graphical representation of the duration of Meiosis I (from the end of diakinesis to the end of anaphase I; Figure S2), Interkinesis, and Meiosis II (prometaphase II to telophase II) calculated from live imaging of anthers in wild type (WT) and *cenh3-4* plants grown at 16, 21, 26 and 30°C. Error bars represent standard deviation (from 16 to 30°C: in wild type n=36,36, 36,46 and *cenh3-4* n=35,24,24,4, *resp.*). (B) Anther loculi in the tetrad stage of wild type (WT), *cenh3-4* and *spo11-2-3* plants grown at 16, 21, 26 and 30°C. Blue arrows indicate examples of produced micronuclei. Scale bar=10 µm. (C) Number of micronuclei per lobe in wild type (WT, n=10,10,10,15), *cenh3-4* (n=14,10,13,10), and *spo11-2-3* (n=19,26,25) plants. Error bars represent standard deviation.

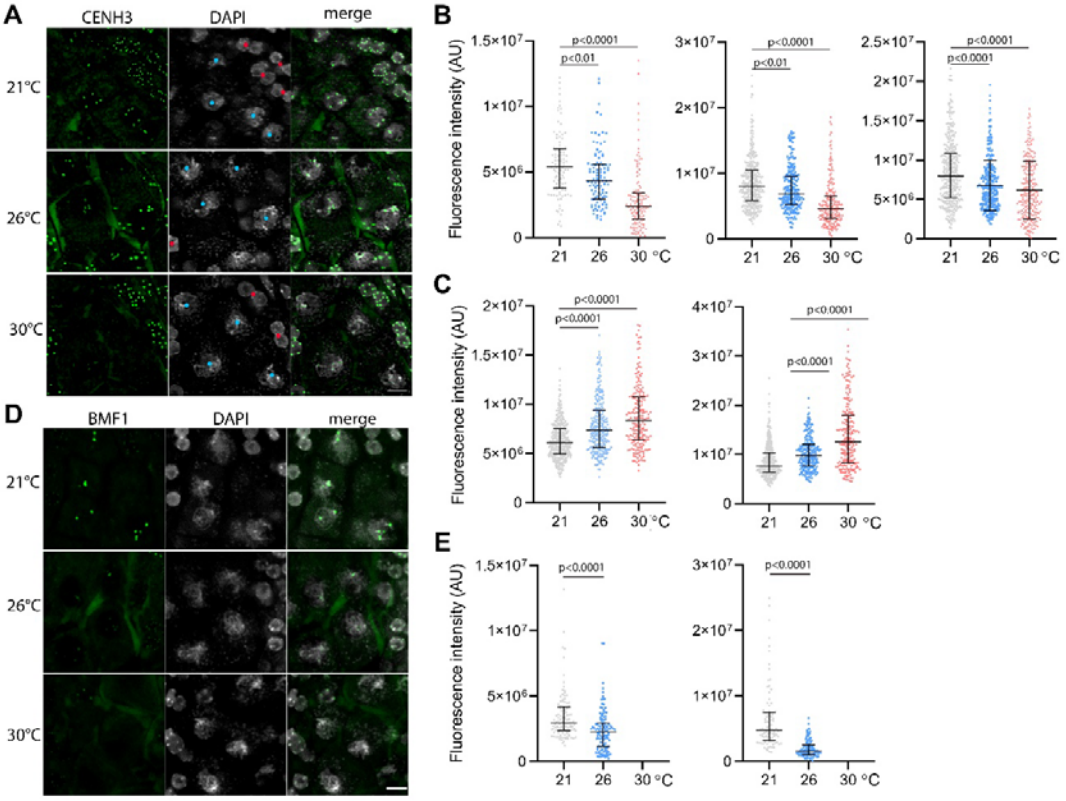

Figure 3. Effect of high temperature on centromere structure in wild type plants.

(A) eYFP:CENH3 expression and DAPI staining of meiotic pachytene (blue dots) and mitotic tapetal cells (red dots) in wild type plants grown at 21, 26 and 30°C. Scale bar=5µm .(B) quantification of CENH3 fluorescence intensity per centromere in pachytene. Each interleaved scatter plot with median and interquartile range shows results of an independent experiment (left graph n=102,103,125, middle n=359,220,233 and right graph n=286,268,233). (C) Quantification of eYFP:CENH3 signal intensity in tapetum cells of plants grown at 21, 26 and 30°C. Each graph represents an independent experiment (left graph n=369,262,233 and right graph n=358,266,213). (D) Expression of BMF1:eYFP in pachytene in plants grown at 21, 26 and 30°C. DNA is counterstained with DAPI. Scale bar=5µm. (E) Quantification of BMF1:eYFP signal intensity per centromere in pachytene in two independent experiments; left graph n=120 and right n=100. Two-tailed t-test is used to depict the significance of the difference.

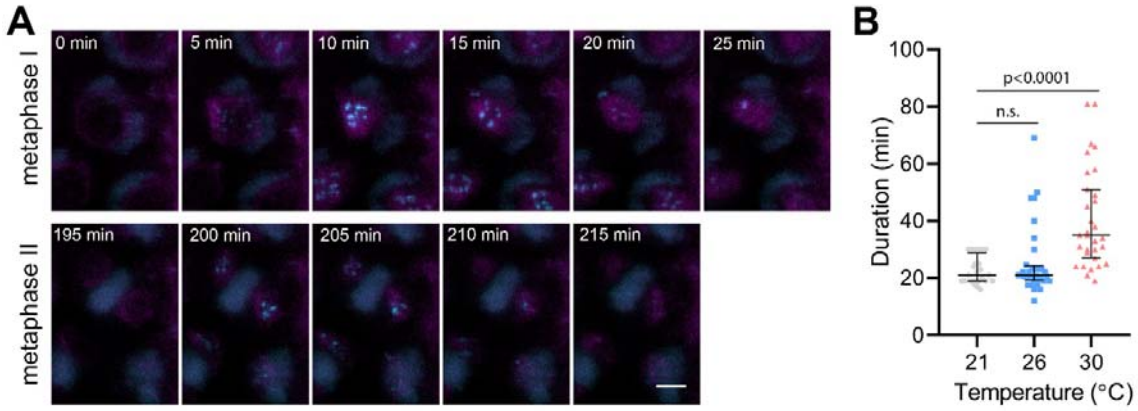

Figure 4. Effect of high temperature on the duration of BMF3:GFP localization during wild type meiosis.

(A) Time lapse series of BMF3:GFP (cyan) and TagRFP:TUB4 (magenta) in PMC from nuclear envelope breakdown to telophase II. Scale bar=5µm. (B) Duration of BMF3:GFP signal in plants grown at 21°C (n=24), 26°C (n=32) and 30°C (n=31). Significance of the difference was calculated via Two-tailed t-test.

Video 1. Live imaging of meiosis in HTA10:RFP chromatin marker in plants grown at 16°C.

Video 2. Live imaging of meiosis in *cenh3-4* plants carrying HTA10:RFP chromatin marker grown at 16°C. Production of micronuclei could be seen in a few PMCs.

Video 3. Live imaging of meiosis in HTA10:RFP chromatin marker in plants grown at 21°C.

Video 4. Live imaging of meiosis in HTA10:RFP chromatin marker in plants grown at 26°C.

Video 5. Live imaging of meiosis in *cenh3-4* plants carrying HTA10:RFP chromatin marker grown at 21°C. Production of micronuclei could be detected in some PMCs.

Video 6. Live imaging of meiosis in *cenh3-4* plants carrying HTA10:RFP chromatin marker grown at 26°C. Production of micronuclei could be detected in most PMCs.

Video 7. Live imaging of meiosis in HTA10:RFP chromatin marker in plants grown at 30°C. Aberrant meiotic products are detected.

Video 8. Live imaging of meiosis in *cenh3-4* plants carrying HTA10:RFP chromatin marker grown at 30°C. Most PMCs undergo aberrant meiotic division and only a few PMCs undergo normal meiotic division resulting in forming unbalanced tetrads.

Video 9. Live imaging of BMF1:eYFP kinetochore marker and HTA10:RFP chromatin marker during meiosis.

Video 10. Live imaging of BMF3:GFP spindle assembly checkpoint marker and TagRFP:TUB4 tubulin marker during both meiosis.

Video 11. Live imaging of BMF3:GFP spindle assembly checkpoint marker and TagRFP:TUB4 tubulin marker during first meiotic division of plants grown at 26°C.

Video 12. Live imaging of BMF3:GFP spindle assembly checkpoint marker and TagRFP:TUB4 tubulin marker during the first meiotic division of plants grown at 30°C.